gels

MDPI

Article

Dipole Theory of Polyzwitterion Microgels and Gels

Murugappan Muthukumar

Department of Polymer Science and Engineering, University of Massachusetts, Amherst, MA 01003, USA; muthu@umass.edu

Abstract: The behavior of polyzwitterions, constituted by dipole-like zwitterionic monomers, is significantly different from that of uniformly charged polyelectrolytes. The origin of this difference lies in the intrinsic capacity of polyzwitterions to self-associate intramolecularly and associate with interpenetrating chains driven by dominant dipolar interactions. Earlier attempts to treat polyzwitterions implicitly assume that the dipoles of zwitterion monomers are randomly oriented. At ambient temperatures, the dipolar zwitterion monomers can readily align with each other generating quadrupoles and other multipoles and thus generating heterogeneous structures even in homogeneous solutions. Towards an attempt to understand the role of such dipolar associations, we present a mean field theory of solutions of polyzwitterions. Generally, we delineate a high-temperature regime where the zwitterion dipoles are randomly oriented from a low-temperature regime where quadrupole formation is significantly prevalent. We present closed-form formulas for: (1) Coil-globule transition in the low-temperature regime, the anti-polyelectrolyte effect of chain expansion upon addition of low molar mass salt, and chain relaxation times in dilute solutions. (2) Spontaneous formation of a mesomorphic state at the borderline between the high-temperature and low-temperature regimes and its characteristics. A universal law is presented for the radius of gyration of the microgel, as a proportionality to one-sixth power of the polymer concentration. (3) Swelling equilibrium of chemically cross-linked polyzwitterion gels in both the high temperature and low-temperature regimes. Addressing the hierarchical internal dynamics of polyzwitterion gels, we present a general stretched exponential law for the time-correlation function of gel displacement vector, that can be measured in dynamic light scattering experiments. The present theory is of direct experimental relevance and additional theoretical developments to all polyzwitterion systems, and generally to biological macromolecular systems such as intrinsically disordered proteins.

Keywords: polyzwitterions; hydrogels; gel swelling equilibria; hierarchical gel dynamics; dipole-dipole interactions; mesomorphic state; polyzwitterion gels

check for updates

Citation: Muthukumar, M. Dipole Theory of Polyzwitterion Microgels and Gels. *Gels* **2024**, *10*, 393. https://doi.org/10.3390/gels10060393

Academic Editors: Fumihiko Tanaka and Chi Wang

Received: 26 April 2024
Revised: 1 June 2024
Accepted: 4 June 2024
Published: 11 June 2024

1. Introduction

Polyzwitterions, where every repeat unit along the chain backbone is a zwitterion (electric dipole) consisting of positive and negative charges separated by designable distance ℓ, exhibit a wide range of material properties in the areas of biolubricants, cosmetics, soft contact lens, etc. [1–10]. Polyzwitterions are known to possess terrific material properties in the areas of cosmetics, soft contact lens, hemodialysis membranes, biolubricants, etc. The self-assembled structures by polyzwitterions hold potential applications. Gels from polyzwitterions are of tremendous use in therapeutic situations involving higher salinity (eye, for example), due to salt-philicity and the enhanced water-holding ability. Control of gel swelling by chemistry in these amphiphilic biocompatible materials can have significant impact. Self-assembly from polyzwitterions can also be of great use in encapsulating a variety of analytes such as drugs and fragrances. Yet, fundamental understanding of their structural organization and functions, such as their enhanced hydro- and salt-philicity in combination with amphiphilicity, is lacking.

In general, the polyzwitterion behavior depends on the dipole density along the chains, dipole length, and identities of the charge of the dipole [11–32], and has attracted significant

theoretical and modeling efforts [33–43]. The rich functional properties of polyzwitterions (polydipoles), that are unprecedented in polyelectrolytes (polymonopoles), originate from delicate cooperative organization of dipolar local charge separations embedded along polymer backbone. The electrostatic forces from dipoles are gentler than the stronger Coulomb forces among monopole charges, resulting in fragility and diversity of local aggregation of zwitterions. The occurrence of dipolar interactions is ubiquitous in many biological macromolecular systems. Almost all protein molecules contain amino acid monomers that can possess either permanent or induced dipole moment. Furthermore, even for the nominal uniformly charged polyelectrolytes such as DNA and sodium poly(styrene sulfonate), dipolar forces are prevalent due to the unavoidable ion-pair formation arising from counterion adsorption on the repeat units. In general, dipole-dipole, charge-charge, and dipole-charge interactions are scripted in these biological as well as synthetic macromolecules resulting in rich complex structural and dynamical behavior. While there has been extensive attention to charge-charge interactions in treating charged macromolecules, the role of dipolar interactions among different parts of the polymer chains and their correlations accompanying physical aggregation is yet be conceptually framed and understood. In this general premise, it is desirable to consider the asymptotic limit of charged macromolecules, where only dipole-dipole interactions are present, as in the case of polyzwitterions. It is thus of fundamental interest to formulate a theoretical platform to account for the role of dipolar forces in polyzwitterions, which is the primary goal of this paper.

Towards a general treatment of effects emanating from zwitterions embedded on polymer backbones, let us first consider different configurations of dipoles (zwitterions) as illustrated in Figure 1. To begin with, the free energy of interaction of two dipoles of moments $\mathbf{p_1}$ and $\mathbf{p_2}$ separated by a distance $\mathbf{r}$ (Figure 1a) in a uniform dielectric medium is given by [1]

$$\Delta F = \frac{1}{4\pi\epsilon_0\epsilon_r}\frac{1}{r^3}[\mathbf{p}_1\cdot\mathbf{p}_2 - 3(\hat{\mathbf{r}}\cdot\mathbf{p}_1)(\hat{\mathbf{r}}\cdot\mathbf{p}_2)], \tag{1}$$

where ϵ_0 is the permittivity of vacuum, ϵ_r is the temperature-dependent dielectric constant of the medium, and the magnitude and unit vector of $\mathbf{r}$ are denoted by r and $\hat{\mathbf{r}}$, respectively. Thus, the interaction between a pair of dipoles depends on their orientations and separation distance. This dipole-dipole interaction is screened in an electrolyte solution. Assuming the validity of the Debye-Hückel theory for electrolyte solutions, the above expression for ΔF is modified to [1]

$$\Delta F = \frac{1}{4\pi\epsilon_0\epsilon}\frac{e^{-\kappa r}}{r^3}\left[(1+\kappa r)\mathbf{p}_1\cdot\mathbf{p}_2 - (3+3\kappa r+\kappa^2 r^2)(\hat{\mathbf{r}}\cdot\mathbf{p}_1)(\hat{\mathbf{r}}\cdot\mathbf{p}_2)\right], \tag{2}$$

where κ is the inverse Debye length (proportional to the square root of concentration c_s of added salt in the solution). For monovalent salts,

$$\kappa^2 = 4\pi\ell_B(c_+ + c_-) = (8000\pi\ell_B N_A)c_s, \tag{3}$$

where c_+ and c_- are the number concentrations of dissociated cations and anions, N_A is the Avogadro number, and ℓ_B is the Bjerrum length defined by

$$\ell_B = \frac{e^2}{4\pi\epsilon_0\epsilon_r k_B T}, \tag{4}$$

with $k_B T$ as the Boltzmann constant times absolute temperature. In the present theory, effects [1] from the finite size of dissociated ions are not accounted for.

If the polyzwitterion solution is dilute and the chain backbone is highly flexible, and if the temperature is high enough in comparison with local dipole-dipole interaction energy, the dipoles of the repeat monomers are expected to be randomly oriented (Figure 1b). The interaction free energy $u_{dd,\text{random}}(r)$ (in units of $k_B T$) between two randomly oriented dipoles with the same dipole moment $pe = \ell e$ (p is dipole length and e is the electronic

charge), separated by distance r in a salty aqueous solution follows from Equation (2) after averaging over orientations of the dipoles as [1]

$$U_{dd,\text{random}}(r) = -\frac{1}{3}\frac{\ell_B^2 p^4}{r^6}e^{-2\kappa r}\left[1 + 2\kappa r + \frac{5}{3}(\kappa r)^2 + \frac{2}{3}(\kappa r)^3 + \frac{1}{6}(\kappa r)^4\right]. \quad (5)$$

If the temperature is not too high and if the salt concentration is not high enough to significantly screen the dipole-dipole interactions, then local pairing of dipoles will result in quadrupoles. There are primarily two orientations of the dipoles forming quadrupoles that are stable, namely the parallel and antiparallel configurations as shown in Figure 1c and Figure 1d, respectively. The distance vector **r** between the centers of the dipoles is along the same direction of the dipole orientations in Figure 1c, whereas it is orthogonal to the directions of the dipoles in Figure 1d. Using Equation (2), the pairwise dipole-dipole interaction energy (in units of $k_B T$) for these two types of quadrupoles is given by

$$U_{dd,\text{parallel}}(r) = -\frac{\ell_B p^2}{r^3}e^{-\kappa r}(2 + 2\kappa r + \kappa^2 r^2), \quad (6)$$

and

$$U_{dd,\text{antiparsallel}}(r) = -\frac{\ell_B p^2}{r^3}e^{-\kappa r}(1 + \kappa r). \quad (7)$$

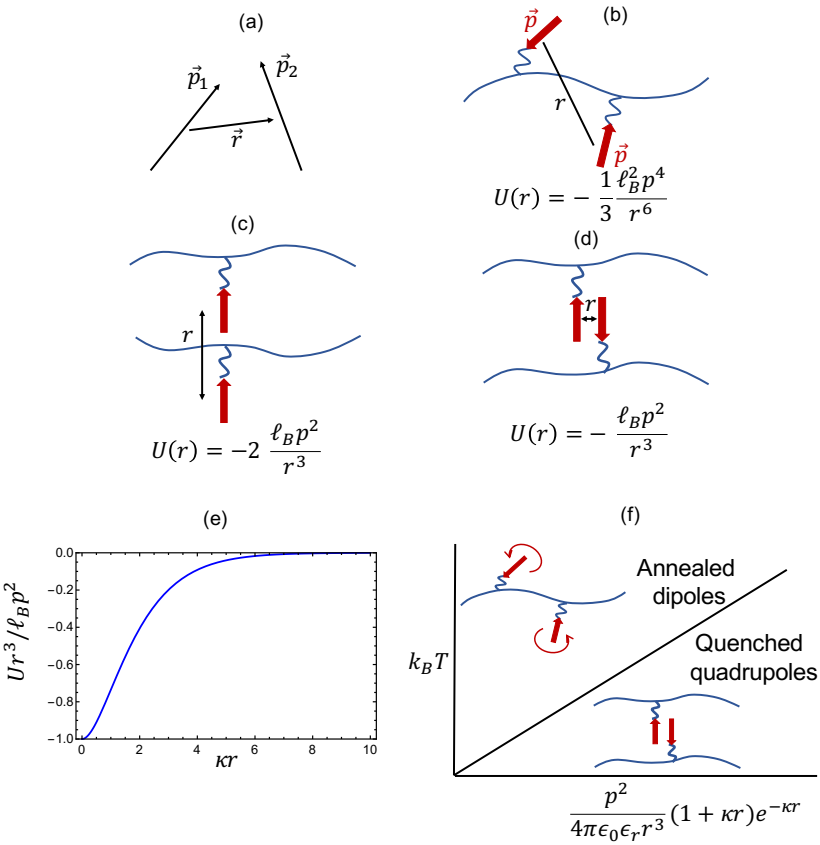

Figure 1. Different scenarios of dipole-dipole interactions as described in the main text. (**a**) Two dipoles $\mathbf{p}_1$ and $\mathbf{p}_2$ separated by a distance **r**. (**b**) Two dipoles of equal dipole moment p are randomly oriented and the interaction energy, $U(r) \sim -1/r^6$ as noted. ℓ_B is the Bjerrum length. (**c**) Parallel orientation of two dipoles with interaction energy $U(r) \sim -1/r^3$. (**d**) Anti-parallel orientation of two dipoles with $U(r) \sim -1/r^3$. (**e**) Weakening of quenched dipole-dipole interaction with an increase in added salt concentration c_s, where the inverse Debye length $\kappa \sim \sqrt{c_s}$. (**f**) Demarkation of the high-temperature and low-tenperature regimes depending on p, r, κ, and the dielectric constant ϵ_r (ϵ_0 = vacuum permittivity).

Even though both parallel and antiprallel dipole orientations are stable, the parallel configuration of dipoles from chain backbones is expected to be considerably less stable (compared to the anti-parallel configuration) due to steric hindrance arising from chain backbone and the inter-dipole distance being much larger and hence weaker because of $1/r^3$ dependence (as sketched in Figure 1c,d). Therefore, it is reasonable to focus only on the anti-parallel arrangement of dipoles for the formation of quadrupoles in polyzwitterions. The strength of $u_{dd,\text{antiprallel}}$ decreases with an increase c_s as illustrated in Figure 1e, where $u_{dd,\text{antiprallel}}$ is plotted against the inverse Debye length $\kappa \sim \sqrt{c_s}$.

At any salt concentration, there exists a threshold temperature $T_{\text{threshold}}$ below which these antiparallel quadrupoles would spontaneously form as essentially quenched configurations, and above which random orientations of dipoles might become plausible. The threshold temperature is obtained from Equations (4) and (7) as

$$T_{\text{threshold}} = \frac{e^2 p^2}{4\pi\epsilon_0\epsilon_r k_B r^3} e^{-\kappa r}(1+\kappa r). \tag{8}$$

As illustrated in Figure 1f, for temperatures higher than $T_{\text{threshold}}$, the polyzwitterion chains behave as an annealed system with random orientation of zwitterions whereas they will form quenched and physically associated quadrupoles for temperatures below $T_{\text{threshold}}$. The value of $T_{\text{threshold}}$ depends on the magnitude of the dipole moment of the zwitterion, dielectric constant, and the salt concentration. Previous theoretical attempts to treat polyzwitterions, with the exception of the author's previous work [35], deal with the high-temperature situation of random orientations of the dipoles. In the present paper, we will address the role of quenched configurations corresponding to the lower part of the diagram in Figure 1f, in addressing polyzwitterion gels. As discussed below, for temperatures above but close to $T_{\text{threshold}}$, the quenched quadrupoles can result in an intermediate mesomorphic microgel formation where the quadrupoles function as physical cross-links and the intervening strands undergo conformational fluctuations with their dipoles being randomly oriented.

The rest of the paper is organized as follows. Defining a continuous Kuhn chain model encompassing chain connectivity and inter-segment dipole-dipole interactions in Section 2, the size and dynamics of isolated polyzwitterion chains are presented in Section 3. Self-assembly of mesomorphic polyzwitterion microgels at $T \geq T_{\text{threshold}}$ is described in Section 4. Swelling equilibrium and hierarchical internal dynamics of polyzwitterion gels are described in Section 5, followed by concluding remarks on the phase behavior of polyzwitterion systems.

2. Model

Consider a system of n polyzwitterion chains each containing N repeat units, n_γ ions of species γ from dissolved salt, and n_s solvent molecules in volume V. Let ℓ and $\mathbf{p}$ be the linear size and dipole moment, respectively, of each zwitterionic repeat unit. Let also the dipole length of the zwitterion be p so that the magnitude of the dipole moment is $|\mathbf{p}| = p\,e$, where the unit charge is explicitly expressed. Representing the polymer chains as continuous curves of contour length $L = N\ell$, the Helmholtz free energy F of the system is given by

$$e^{-\frac{F}{k_B T}} = \frac{1}{n! n_s! \prod_\gamma n_\gamma!} \int \prod_{\alpha=1}^{n} \mathcal{D}[\mathbf{R}_\alpha] \int \prod_{i}^{n_s+\sum_\gamma n_\gamma} d\mathbf{r}_i$$
$$\times \exp\{-\frac{3}{2\ell^2}\sum_{\alpha=1}^{n}\int_0^N ds_\alpha (\frac{\partial \mathbf{R}_\alpha(s_\alpha)}{\partial s_\alpha})^2 - \frac{1}{2}\sum_{\alpha=1}^{n}\sum_{\beta=1}^{n}\int_0^N ds_\alpha \int_0^N ds_\beta U_{pp}[\mathbf{R}_\alpha(s_\alpha) - \mathbf{R}_\beta(s_\beta)]$$
$$-\sum_{\alpha=1}^{n}\int_0^N ds_\alpha \sum_{i=1}^{n_s} U_{ps}[\mathbf{R}_\alpha(s_\alpha) - \mathbf{r}_i] - \frac{1}{2}\sum_{i=1}^{n_s}\sum_{j=1}^{n_s} U_{ss}(\mathbf{r}_i - \mathbf{r}_j)$$

$$-\sum_{\alpha=1}^{n}\int_0^N ds_\alpha \sum_{i=1}^{\sum_\gamma n_\gamma} U_{pi}[\mathbf{R}_\alpha(s_\alpha)-\mathbf{r}_i]-\frac{1}{2}\sum_{i=1}^{\sum_\gamma n_\gamma}\sum_{j=1}^{\sum_\gamma n_\gamma} U_{ij}(\mathbf{r}_i-\mathbf{r}_j)\}. \tag{9}$$

Here $\mathbf{R}_\alpha(s_\alpha)$ is the position vector of the arc length variable $s_\alpha(0 \le s_\alpha \le N)$ of the α-th chain. $U_{pp}(\mathbf{r})$ is the interaction energy between two repeat units of the chains separated by a distance $\mathbf{r}$,

$$U_{pp}(\mathbf{r}) = v_{pp}\ell^3\delta(\mathbf{r}) + v_{dipole}(\mathbf{r}), \tag{10}$$

where v_{pp} is the short-ranged monomer-monomer excluded volume interaction parameter, and $\delta(\mathbf{r})$ is the Dirac delta function. v_{pp} represents only two-body interactions, and three-body interactions need to be included in describing situations where polyzwitterion chains form globule-like structures. $v_{dipole}(\mathbf{r})$ is the dipole-dipole interaction that depends on specific dipole orientations as displayed in Figure 1.

The short-ranged interactions between polymer repeat units and solvent molecules and between solvent molecules are given by

$$U_{ps}(\mathbf{r}) = v_{ps}\ell^3\delta(\mathbf{r}) \qquad \text{and} \qquad U_{ss}(\mathbf{r}) = v_{ss}\ell^3\delta(\mathbf{r}), \tag{11}$$

where v_{ps} and v_{ss} are parameters analogous to v_{pp}. The electrostatic interactions between dissociated monovalent ions and between dipoles and ions are given by

$$U_{ij}(\mathbf{r}) = \frac{z_i z_j \ell_B}{r} \qquad \text{and} \qquad U_{pi}(\mathbf{r}) = \frac{z_i}{e}\frac{\ell_B}{r^3}(\mathbf{p}\cdot\mathbf{r}), \tag{12}$$

where $z_i e$ is the charge of the i-th dissociated ion, $\mathbf{p}$ is the dipole moment of the repeat unit, and $r = |\mathbf{r}|$.

Integrating out all degrees of freedom associated with mobile salt ions and solvent molecules within the framework of the Debye-Hückel theory, we get

$$e^{-\frac{F}{k_BT}} = e^{-\frac{F_0}{k_BT}}\frac{1}{n!}\int\prod_{\alpha=1}^{n}\mathcal{D}[\mathbf{R}_\alpha]\exp\{-\frac{3}{2\ell^2}\sum_{\alpha=1}^{n}\int_0^N ds_\alpha(\frac{\partial\mathbf{R}_\alpha(s_\alpha)}{\partial s_\alpha})^2$$
$$-\frac{1}{2}\sum_{\alpha=1}^{n}\sum_{\beta=1}^{n}\int_0^N ds_\alpha\int_0^N ds_\beta U[\mathbf{R}_\alpha(s_\alpha)-\mathbf{R}_\beta(s_\beta)]\} \tag{13}$$

Here F_0 is the free energy of the background fluid where the polyzwitterions are present. It arises from the translational entropy of dissociated salt ions and solvent and the charge fluctuations from the salt ions, given by

$$\frac{F_0}{k_BTV} = c_0\ln c_0 - c_0 + \sum_i(c_i\ln c_i - c_i) - \frac{\kappa^3}{12\pi}, \tag{14}$$

where c_0 and c_i are the number concentrations of the solvent and i-th electrolyte ion. In Equation (12),

$$U(\mathbf{r}) = v\ell^3\delta(\mathbf{r}) + v_{dipole-dipole}(\mathbf{r},\kappa), \tag{15}$$

where v is the familiar excluded volume parameter, written equivalently as $(1-2\chi)$, where χ is the Flory-Huggins parameter to compound polymer-polymer, polymer-solvent, and solvent-solvent short-ranged interactions. The dipole contribution to $U(\mathbf{r})$ is $v_{dipole-dipole}(\mathbf{r})$, as explicitly given in Equations (2)–(6). In the situation of anti-parallel orientations of two adjacent dipoles with a separation distance r_0 comparable to the monomer size ℓ, $v_{dipole-dipole}(\mathbf{r})$ can be written as a delta function (analogous to the treatment of the excluded volume interaction) given by

$$v_{dipole-dipole}(\mathbf{r}) = v_d\delta(\mathbf{r}), \tag{16}$$

with

$$v_d = -\frac{f\ell_B p^2}{r_0^3} e^{-\kappa r_0}(1+\kappa r_0), \tag{17}$$

where we introduce the probability f of realizing anti-parallel orientations of the dipoles of two adjacent zwitterions. Considering only the favored orientations (Figure 1c,d), f is 0.5, if the dipoles are completely free without any entropic contribution from chain connectivity. In realistic situations, we expect f to be smaller than this value. For example, based only on the loss of orientational entropy of a dipole to be oriented in a specified direction, $f = 1/4\pi$. Combining Equations (15) and (17), we define an effective interaction parameter,

$$v_{eff} = v + v_d = (1-2\chi) - \frac{f\ell_B p^2}{r_0^3} e^{-\kappa r_0}(1+\kappa r_0). \tag{18}$$

Hence, the χ parameter specific to polymer-solvent pair without zwitterions, is increased by an amount proportional to $\ell_B p^2$.

We note that the expression for v_{eff} is quite different for the high temperature situation (upper part of Figure 1f) corresponding to randomly oriented dipoles. In this situation, v_{eff} becomes [1]

$$v_{eff} = v + v_{dd}, \tag{19}$$

where

$$v_{dd} = -\frac{\pi}{9}\frac{\ell_B^2 p^4}{\ell^6} e^{-2\kappa\ell}\left[4 + 8\kappa\ell + 4(\kappa\ell)^2 + (\kappa\ell)^3\right]. \tag{20}$$

Here the dipole contribution is proportional to $\ell_B^2 p^4$, instead of $\ell_B p^2$ in Equation (17).

3. Size and Dynamics of Polyzwitterions in Dilute Solutions

3.1. Size: Anti-Polyelectrolyte Effect

For an isolated polyzwitterion chain, the probability distribution function $G(\mathbf{R}, N)$ for a chain of N repeat units and end-to-end distance $\mathbf{R}$ follows from Equations (9)–(20) as

$$G(\mathbf{R},N) = \int_{\mathbf{0}}^{\mathbf{R}} \mathcal{D}[\mathbf{R}(s)] \exp\{-\frac{3}{2\ell^2}\int_0^N ds(\frac{\partial \mathbf{R}(s)}{\partial s})^2 - \frac{\ell^3}{2}\int_0^N ds \int_0^N ds' v_{eff}\delta[\mathbf{R}(s)-\mathbf{R}(s')]$$
$$-\ell^6 w \int_0^N ds \int_0^N ds' \int_0^N ds'' \delta[\mathbf{R}(s)-\mathbf{R}(s')]\delta[\mathbf{R}(s')-\mathbf{R}(s'')], \tag{21}$$

where the three-body interaction of strength w is included in anticipation of the necessity to stabilize the expected globular state of the polyzwitterion chain. The free energy F_1 and the mean square end-to-end distance $\langle R^2 \rangle$ of the chain are given by $G(\mathbf{R}, N)$ as

$$\frac{F_1}{k_B T} = -\ln \int d\mathbf{R}\, G(\mathbf{R}, N), \tag{22}$$

and

$$\langle R^2 \rangle = \frac{\int d\mathbf{R}\, R^2\, G(\mathbf{R}, N)}{\int d\mathbf{R}\, G(\mathbf{R}, N)}. \tag{23}$$

We will use the variational procedure [44], which has been found to be effective in treating polyelectrolytes and neutral polymers, to calculate F_1 and $\langle R^2 \rangle$ in terms of χ, ℓ_B, p, and c_s. Since the technical details of this procedure are already in the literature [1,44], we give only the results for F_1 and $\langle R^2 \rangle$ along with the effect of dipoles on the theta θ temperature relevant to phase behavior.

3.1.1. Designing θ Temperature

Writing v_{eff} of Equation (18) as $(1 - 2\chi_{eff})$, we get

$$1 - 2\chi_{eff} = 1 - 2\chi - \frac{f\ell_B p^2}{r_0^3} e^{-\kappa r_0}(1 + \kappa r_0), \tag{24}$$

so that

$$\chi_{eff} = \chi + \frac{1}{2}\frac{f\ell_B p^2}{r_0^3} e^{-\kappa r_0}(1 + \kappa r_0). \tag{25}$$

Hence a plot of χ_{eff} versus $\ell_B p^2/\ell^3$ is linear with the slope depending on salt concentration as shown in Figure 2a. If the polyzwitterion solution exhibits upper solution critical solution temperature (UCST) behavior, as prescribed by $\chi = \theta/2T$, the dependence of θ temperature (now θ_{eff}) on the dipole length of the zwitterion is given by

$$\theta_{eff} = \theta + \frac{fe^2 p^2 e^{-\kappa r_0}(1 + \kappa r_0)}{4\pi\epsilon_0\epsilon_r k_B r_0^3}, \tag{26}$$

where the definition of ℓ_B is used. The elevation of the theta temperature is linearly proportional to p^2 with the coefficient being a decreasing function of c_s. Thus the dipole length p of the zwitterion has a significant effect on the θ temperature of polyzwitterion solutions and offers an important synthesis tool to design the phase behavior of polyzwitterions.

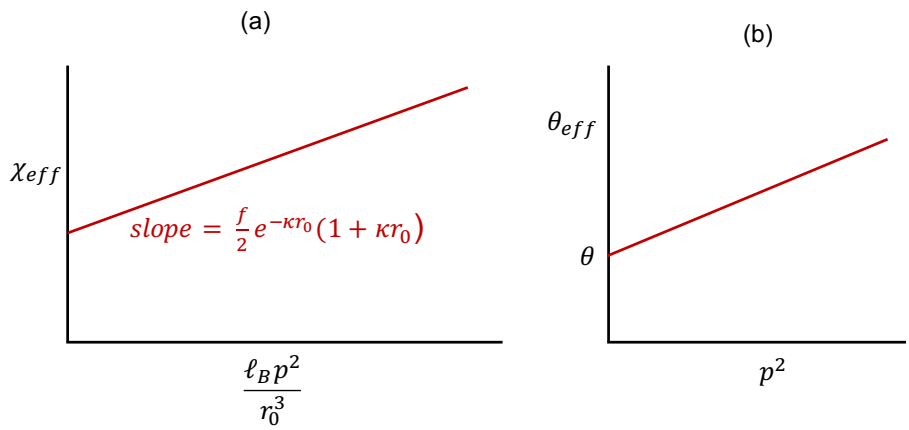

Figure 2. Elevation of θ temperature by p^2. (**a**) Effective chi parameter and (**b**) effective theta temperature.

3.1.2. Size and Free Energy

Using the variational procedure and following the derivation in Refs. [1,44], the free energy F_1 of a single polyzwitterion chain in solutions is obtained from Equation (22) as

$$\frac{F_1}{k_B T} = \frac{3}{2}\left[\frac{R^2}{N\ell^2} - 1 - \ln\left(\frac{R^2}{N\ell^2}\right)\right] + \frac{4}{3}\left(\frac{3}{2\pi}\right)^{3/2}(v + v_d)\frac{N^2\ell^3}{R^3} + w\frac{N^3\ell^6}{R^6}, \tag{27}$$

where the unknown three-body interaction parameter w absorbs all numerical prefactors. By minimizing the above free energy expression with respect to the root mean square end-to-end distance R, $dF_1(R)/dR = 0$, we get

$$\left(\frac{R^2}{N\ell^2}\right)^{5/2} - \left(\frac{R^2}{N\ell^2}\right)^{3/2} = \frac{4}{3}\left(\frac{3}{2\pi}\right)^{3/2}(v + v_d)\sqrt{N} + 2w\left(\frac{N\ell^2}{R^2}\right)^{3/2}. \tag{28}$$

Rewriting this result in terms of the chain expansion factor $\alpha = (R^2/N\ell^2)^{1/2}$, we obtain

$$\alpha^5 - \alpha^3 - \frac{2w}{\alpha^3} = \frac{4}{3}\left(\frac{3}{2\pi}\right)^{3/2}(v + v_d)\sqrt{N}. \tag{29}$$

A plot of α versus the term on the right-hand-side of this equation is given in Figure 3a exhibiting the coil-globule transition.

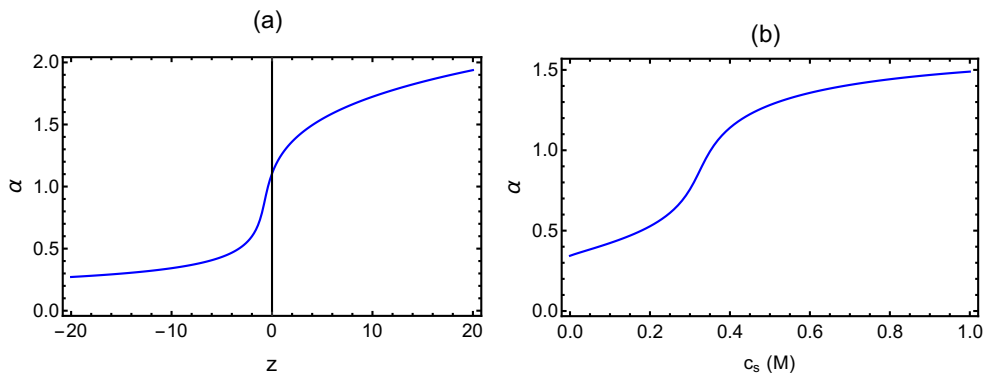

Figure 3. (**a**) Coil-globule transition: α is the chain expansion factor and $z = \frac{4}{3}(\frac{3}{2\pi})^{3/2}(v + v_d)\sqrt{N}$. (**b**) Anti-polyelectrolyte effect.

Since the dipole-dipole interactions are attractive ($v_d < 0$), polyzwitterions can readily form globules for sufficiently large dipole lengths. In addition to the dipole length, c_s plays an important role in determining the dipole-dipole interaction strength. Once a polyzwitterion forms a globule in the low salt condition, it expands upon weakening the inter-segment dipole-dipole attraction with additional salt. This behavior of formation of expanded coil from a globule upon addition of salt is illustrated in Figure 3b, where the chain expansion factor α is plotted versus c_s for $v = 1, N = 225, w = 0.2$, and $f\ell_B p^2/r_0^3 = 2.5$. This behavior is the opposite to the familiar polyelectrolyte behavior where the size shrinks due to the screening of charge-charge repulsion with added salt. The 'anti-polyelectrolyte' behavior of polyzwitterion chains arises from screening of the attractive dipole-dipole interaction with added salt. The extreme limits of formation of globule and coil structures and the intervening crossover behavior are given by Equation (29). The size and free energy of the coil and globule states predicted by Equations (27) and (28) are as follows.

(a) Polyzwitterion coils ($v + v_d > 0$):

For sufficiently large positive values of $v + v_d$, Equation (28) gives

$$\left(\frac{R^2}{N\ell^2}\right)^{5/2} = \frac{4}{3}\left(\frac{3}{2\pi}\right)^{3/2}(v + v_d)\sqrt{N}, \tag{30}$$

so that the root-mean-square end-to-end distance R, which is proportional to the radius of gyration R_g, scales with the degree of polymerization N as

$$\frac{R_g}{\ell} \sim (v + v_d)^{1/5}N^{3/5}, \tag{31}$$

with the size exponent $\nu = 3/5$. This result is as expected for good solution conditions. Substituting this result in Equation (27), the free energy F_1 is given by

$$\frac{F_1}{k_B T} = 1.8(v + v_d)^{2/5}N^{1/5}. \tag{32}$$

(b) Polyzwitterion globules ($v + v_d < 0$): For sufficiently strong attractive dipole-dipole interactions ($v + v_d < 0$), Equation (28) gives

$$\left(\frac{R^2}{N\ell^2}\right)^{3/2} = \left[\frac{4}{3}\left(\frac{3}{2\pi}\right)^{3/2}|v + v_d|\right]^{-1}\frac{2w}{\sqrt{N}}, \tag{33}$$

so that

$$\frac{R}{\ell} = \left[\frac{3}{2}(\frac{2\pi}{3})^{3/2}\frac{w}{|v + v_d|}\right]^{1/3} N^{1/3}. \tag{34}$$

Hence the scaling behavior of R_g of polyzwitterion globule is

$$\frac{R_g}{\ell} \sim \left(\frac{w}{|v + v_d|}\right)^{1/3} N^{1/3}, \tag{35}$$

with the size exponent $\nu = 1/3$, as expected for globules.

Substituting Equation (34) into Equation (27), the free energy of the globule is given as

$$\frac{F_1}{k_B T} = \frac{9}{2\pi^3}\frac{|v + v_d|^2}{w}N. \tag{36}$$

3.2. Dynamics

The Rouse equation for the dynamics of the position $\mathbf{R}_m(t)$ of the m-th segment at time t, applicable in the absence of hydrodynamic interaction, is given as [1,45]

$$\zeta_b\frac{\partial \mathbf{R}_m(t)}{\partial t} - \frac{3k_B T}{\ell^2}\frac{\partial^2 \mathbf{R}_m(t)}{\partial m^2} + \frac{\partial}{\partial \mathbf{R}_m}\sum_j U(\mathbf{R}_m - \mathbf{R}_j) = \mathbf{f}_m(t), \tag{37}$$

where ζ_b is the segment friction coefficient, U is the intersegment interactions (Equation (9)), and $\mathbf{f}_m$ is the random force acting on the m-th segment. By approximately linearizing the nonlinear dependence of U on $\mathbf{R}_m(t)$ in terms of an effective Kuhn length ℓ_{eff}, Equation (37) is approximated as [1]

$$\zeta_b\frac{\partial \mathbf{R}_m(t)}{\partial t} - \frac{3k_B T}{\ell\ell_{\text{eff}}}\frac{\partial^2 \mathbf{R}_m(t)}{\partial m^2} = \mathbf{f}_m(t), \tag{38}$$

where ℓ_{eff} is related to the chain expansion factor α as $\ell_{\text{eff}}/\ell = \alpha^2$ with $\langle R^2\rangle = N\ell\ell_{\text{eff}}$. In general, since $\langle R^2\rangle \sim N^{2\nu}$,

$$\ell_{\text{eff}} \sim N^{2\nu-1}. \tag{39}$$

Introducing the Fourier transform of $\mathbf{R}_m(t)$ in terms of the Rouse modes $\hat{R}_p(t)$ (where p denotes the Rouse mode index),

$$\mathbf{R}(m,t) = \sum_{p=-\infty}^{\infty}\hat{R}_p(t)\cos\left(\frac{\pi p m}{N}\right), \tag{40}$$

$$\hat{R}_p(t) = \frac{1}{N}\int_0^N dm\,\mathbf{R}(m,t)\cos\left(\frac{\pi p m}{N}\right), \tag{41}$$

we get

$$\zeta_b\frac{\partial \hat{R}_p(t)}{\partial t} + \frac{3\pi^2 k_B T}{\ell\ell_{\text{eff}}}\left(\frac{p}{N}\right)^2\hat{R}_p(t) = \hat{f}_p(t), \qquad \text{(Rouse)} \tag{42}$$

where

$$\ell_{\text{eff}} \sim \left(\frac{\pi p}{N}\right)^{1-2\nu}. \tag{43}$$

The dependence of the relaxation time τ_p of the p-th Rouse mode is obtained from Equation (42) as

$$\tau_p = \frac{\zeta_b \ell \ell_{\text{eff}}}{3\pi^2 k_B T}\left(\frac{N}{p}\right)^2 \sim \frac{\zeta_b}{T}\left(\frac{N}{p}\right)^{2\nu+1}. \tag{44}$$

The longest chain relaxation time τ_R (Rouse time) corresponding to $p = 1$ scales as

$$\tau_R \sim N^{2\nu+1} \qquad \text{(Rouse)} \tag{45}$$

According to the Rouse dynamics, the time correlation function of the end-to-end distance vector $\mathbf{X}(t) = \mathbf{R}_N(t) - \mathbf{R}_0(t)$ is known as [45]

$$\langle \mathbf{X}(t) \cdot \mathbf{X}(0) \rangle = \langle R^2 \rangle (\frac{8}{\pi^2}) e^{-t/\tau_R} \sim e^{-A_R t/N^{2\nu+1}}, \qquad \text{(Rouse)} \tag{46}$$

where A_R is the prefactor in Equation (44). The above equation is derived using the assumption that the longest relaxation time ($p = 1$ mode) dominates the time correlation function of the end-to-end distance.

When hydrodynamic interaction is fully present as in dilute solutions, Equation (42) is modified into the Zimm description [1],

$$\frac{\partial \hat{R}_p(t)}{\partial t} + D_p \frac{3\pi^2 k_B T}{\ell \ell_{\text{eff}}}\left(\frac{p}{N}\right)^2 \hat{R}_p(t) = \frac{\hat{f}_p(t)}{\zeta_b}. \qquad \text{(Zimm)} \tag{47}$$

Here, D_p is the preaveraged hydrodynamic interaction tensor for all chain segments given as

$$D_p \sim \frac{1}{\eta_0}\left(\frac{\pi p}{N}\right)^{\nu-1}. \tag{48}$$

The Zimm relaxation time of the p-th Rouse mode follows from Equation (47) as

$$\tau_{p,\text{Zimm}} = \frac{\ell \ell_{\text{eff}}}{3\pi^2 k_B T}\frac{1}{D_p}\left(\frac{N}{p}\right)^2. \tag{49}$$

Using Equations (43) and (48),

$$\tau_{p,\text{Zimm}} \sim \frac{\eta_0}{T}\left(\frac{N}{p}\right)^{3\nu}, \tag{50}$$

so that the longest relaxation time τ_Z (Zimm time) is

$$\tau_Z \sim N^{3\nu}. \qquad \text{(Zimm)} \tag{51}$$

Analogous to Equation (46), the time correlation function of the end-to-end distance vector $\mathbf{X}(t)$ with hydrodynamic interaction present is given by

$$\langle \mathbf{X}(t) \cdot \mathbf{X}(0) \rangle \sim e^{-t/\tau_Z} \sim e^{-A_Z t/N^{3\nu}}. \qquad \text{(Zimm)} \tag{52}$$

The above results on polyzwitterion single chains are used below in arriving at mean field predictions of microgel formation and internal dynamics of gels in polyzwitterion systems.

4. Polyzwitterion Microgels in Solutions

For polyzwitterion concentrations above the overlap concentration, the chains interpenetrate and intermingle. For such semidilute concentrations, the solution is uniform if there are no driving forces for local aggregation. in the case of polyzwitterions, such a scenario is feasible only in the high temperature phase in Figure 1f where the zwitterion dipoles are randomly oriented. On the other hand, in the low temperature phase (bottom in Figure 1e), the stable quenched quadrupoles are expected to result in pervasive network formation with local heterogeneous structures and macrophase separation. At intermediate conditions for $T \geq T_{threshold}$, we anticipate formation of physical aggregation into microgels.

We label this situation as the mesomorphic state since it emerges as an interlude between homogeneous liquid phase and liquid-liquid or liquid-gel macrophase separation. In the mesomorphic state of polyzwitterion solutions, most of the zwitterion dipoles are randomly oriented with the rest of them are anchored into quadrupoles. The quadrupole energy can be quite high compared to the thermal energy. As an example, for $\ell = 1$ nm, $p = 1$ nm, $\ell_B = 0.7$ nm, and the inter-dipole distance $r_0 = 0.25$ nm, the quadrupole energy u (Figure 1e) is $64k_BT$. If u is so strong, the various quadrupoles will act like physical cross-links and the intervening strands behave like flexible chains with intra-strand excluded volume interactions and randomly oriented dipole-dipole interactions.

We address this mesomorphic state by the following approach. (a) Using combinatorics and the pioneering works of Tanaka [46] and Semenov and Rubinstein [47] on associating polymers, we present the equation of state for the fraction of dipoles involved in quadrupole formation. (b) Using Flory's mean field theory [48–52] of swollen networks, swelling equilibrium of polyzwitterion gels is derived. (c) Specializing on microgels formed by finite number of polyzwitterion chains, their free energy is derived. (d) Using the free energies of isolated chains and microgels containing prescribed number of chains, an the classical micellization/aggregation theory [53], the critical aggregation concentration (CAC) and microgel size distribution are derived.

4.1. Equation of State for Quadrupole Formation

For a solution of volume V_0 containing n polyzwitterion chains, each with N repeat units of volume v_0, the total number of dipoles capable of quadrupole formation is

$$N_s = fnN = f\phi_0 \frac{V_0}{v_0}, \tag{53}$$

where f is the fraction of monomers that have the correct orientation for the formation of quadrupoles, and $\phi_0 = nNv_0/V_0$ is the volume fraction of polyzwitterion. Let q be the fraction of dipoles associated as quadrupoles so that the number of physical crosslinks N_c is given as

$$N_c = \frac{q}{2} fnN = \frac{q}{2} N_s. \tag{54}$$

The free energy F_0 of the cross-linked Gaussian network is

$$\frac{F_0}{k_BT} = -\ln Z_0, \tag{55}$$

where the partition function Z_0 is given by

$$Z_0 = Q_1 Q_2 Q_3 e^{\epsilon N_c}, \tag{56}$$

where Q_1, Q_2, and Q_3 are, respectively, the probability to choose $2N_c$ dipoles out of N_s dipoles, the probability of forming N_c quadrupoles out of $2N_c$ dipoles, and the probability of finding two dipoles closeby. ϵ is the energy gain in the formation of one quadrupole. Q_1, Q_2, and Q_3 are given by

$$Q_1 = \frac{N_s!}{(2N_c)!(N_s - 2N_c)!}, \quad Q_2 = (2N_c - 1)(2N_c - 3)\cdots 3 \cdot 1, Q_3 = \left(\frac{v_0}{V_0}\right)^{N_c}. \tag{57}$$

Substituting Equations (56) and (57) in Equation (55), and using the Stirling approximation, we get

$$\frac{F_0}{k_BT} = -\left(\frac{v_0}{V_0}\right)\left[\frac{fq\phi_0}{2}\ln\left(\frac{f\phi_0}{e}\right) - \frac{f\phi_0}{2}[q\ln q + 2(1-q)\ln(1-q) - \epsilon q]\right]. \tag{58}$$

Minimizing F_0 with respect to q, $\partial F_0/\partial q = 0$, we get the equation of state for the optimal fraction of dipoles associated into quadrupoles as

$$\frac{q}{(1-q)^2} = f\phi_0 e^{\epsilon}. \tag{59}$$

This expression is equivalent to the previous results of Semenov and Rubinstein [47], and the chemical equilibrium expression of Tanaka [46].

4.2. Swelling Equilibrium of Polyzwitterion Gels

We assume that the free energy F of a gel made from n chains (of N monomers) is the additive sum of free energy F_{el} due to elasticity, free energy of mixing F_{mix}, free energy F_{elec} due to electrostatic interactions among randomly oriented dipoles, and free energy F_{quad} due to formation of quadrupoles,

$$F = F_{el} + F_{mix} + F_{elec} + F_{quad}. \tag{60}$$

The free energy F_{el} from the elasticity of the gel is obtained from the earlier works of Flory, Dusek and Patterson, and Tanaka [48–52]. Given that there are $2N_c$ monomers involved in quadrupoles (crosslinks) out of the total $N_0 = nN$ monomers in the system, the number of monomers per cross-linked unit, N_e, is

$$N_e = \frac{N_0}{2N_c} = \frac{nN}{2N_c}. \tag{61}$$

Adopting the Flory-Stockmayer assumption that the cross-linking statistics is that of tree-like network architecture, the number of elastically effective chain strand (n_{eff}) is

$$n_{eff} = 2N_c(1 - \frac{2N_c}{N}). \tag{62}$$

Approximating this result,

$$n_{eff} \simeq 2N_c = \frac{nN}{N_e} = \frac{n}{\gamma}, \tag{63}$$

where Equation (61) is used and $\gamma = N_e/N$. Thus there are n_{eff} elastically active strands of N_e monomers and $N_c = n_{eff}/2$ crosslinks.

It is noteworthy to point out that the minimum value of N, N_{min}, required for network formation depends inversely on the fraction q of dipoles associated as quadrupoles. Since $N_c = qfnN/2$ (Equation (54)),

$$N_e = \frac{nN}{2N_c} = \frac{1}{qf}, \tag{64}$$

so that $N_{min} = N_e$ given as

$$N_{min} == \frac{1}{qf}, \tag{65}$$

where the equilibrium value of q is given in Equation (59).

For an isotropically swollen gel of swelling ratio $\lambda = V/V_0$ (where V is the volume of the swollen gel and V_0 is the gel volume in its reference state of Gaussian network), the standard theory of rubber elasticity gives

$$\frac{F_{el}}{k_B T} = \frac{3}{2} n_{eff}(\lambda^2 - 1 - \ln\lambda). \tag{66}$$

The volume fraction of the polyzwitterion in the swollen gel is

$$\phi = \frac{V_d}{V} = \frac{V_d}{V_0} = \phi_0 \frac{1}{\lambda^3}, \tag{67}$$

where V_d is the volume of dry polyzwitterion material and $\phi_0 = V_d/V_0$. Taking $V_d = nNv_0$ and V_0 as the value given by the volume of Gaussian coils proportional to $N^{3/2}$,

$$\phi_0 = \frac{nNv_0}{n(4\pi R_{g0}^3/3)} = \frac{a}{\sqrt{N}}, \tag{68}$$

where a is a constant of order one. In view of $\gamma = N_e/N$,

$$\phi_0 = a\sqrt{\frac{\gamma}{N_e}}. \tag{69}$$

By combining Equations (66) and (67), F_{el} is given by

$$\frac{F_{el}}{k_BT} = \frac{3}{2}n_{eff}\left[(\frac{\phi_0}{\phi})^{2/3} - 1 + \frac{1}{3}\ln(\frac{\phi_0}{\phi})\right]. \tag{70}$$

For $\phi \ll 1$, this expression reduces to

$$\frac{F_{el}}{k_BT} = \frac{3}{2}n_{eff}(\frac{\phi_0}{\phi})^{2/3}. \tag{71}$$

The classical expression for for the free energy of mixing for a gel is

$$\frac{F_{mix}}{k_BT} = (\frac{V}{v_0})[(1-\phi)\ln(1-\phi) + \chi\phi(1-\phi)], \tag{72}$$

where ϕ refers to $n_{eff}N_ev_0/V$.

The electrostatic contribution from randomly oriented zwitterion dipoles to the free energy is

$$\frac{F_{elec}}{k_BT} = \frac{\ell^3}{2}\sum_{\alpha}^{n_{eff}}\sum_{\beta}^{n_{eff}}\int_0^{N_e} ds_\alpha \int_0^{N_e} ds_\beta\, v_{dd}\, \delta[\mathbf{R}(s_\alpha) - \mathbf{R}(s_\beta)],$$

where mean field approximation is used and v_{dd} is given in Equation (20). Combining F_{mix} and F_{elec}, we get

$$\frac{F_{mix}}{k_BT} + \frac{F_{elec}}{k_BT} = \frac{V}{v_0}\left[(1-\phi)\ln(1-\phi) + \chi\phi - \chi_{eff}\phi^2\right], \tag{73}$$

where χ_{eff} now is

$$\chi_{eff} = \chi - v_{dd}/2. \tag{74}$$

For $\phi \ll 1$,

$$\frac{F_{mix}}{k_BT} + \frac{F_{elec}}{k_BT} = n_{eff}N_e\left[(\frac{1}{2} - \chi_{eff})\phi + O(\phi^2)\right] + \text{constant}. \tag{75}$$

The free energy due to quadrupole formation is

$$\frac{F_{quad}}{k_BT} = -N_c\epsilon = -\frac{n_{eff}}{2}\epsilon \tag{76}$$

Collecting the results for $F_{el}, F_{mix}, F_{elec}$, and F_{quad} from Equations (71), (75) and (76), we get the free energy of a gel with n_{eff} elastically active strands as

$$\frac{F_{n_{eff}}}{k_BTn_{eff}} = -\frac{\epsilon}{2} + N_e\left(\frac{1}{2} - \chi_{eff}\right)\phi + \frac{3}{2}\left(\frac{\phi_0}{\phi}\right)^{2/3}. \tag{77}$$

The minimization of this expression with respect to ϕ yields the polyzwitterion volume fraction at the swelling equilibrium of the polyzwitterion gel as

$$\phi = \frac{\phi_0^{2/5}}{N_e^{3/5}(\frac{1}{2} - \chi_{eff})^{3/5}}. \tag{78}$$

Using Equation (68), we get

$$\phi = \frac{a^{2/5}\gamma^{1/5}}{N_e^{4/5}(\frac{1}{2} - \chi_{eff})^{3/5}}. \tag{79}$$

Substituting this result in Equation (77), we obtain

$$\frac{F_{n_{eff}}}{k_B T n_{eff}} = -\frac{\epsilon}{2} + \frac{5}{2}a^{2/5}\gamma^{1/5}\left(\frac{1}{2} - \chi + \frac{v_{dd}}{2}\right)^{2/5} N_e^{1/5} + \text{constant}. \tag{80}$$

4.3. Equilibrium Distribution of Microgel Size

Since we know expressions for the free energies of isolated chains and microgels containing a certain number of polyzwitterion chains, albeit using mean field arguments, we can derive the distribution of number of polyzwitterion chains in aggregates as a function of the characteristics of the zwitterion dipoles, and salt concentration for $T \geq T_{threshold}$. According to the standard theory [53] of micellization/aggregation, the mole fraction X_m of aggregates with m elastically effective strands ($mN_e = nN$) is given as

$$X_m = m\left[X_1 e^{(F_1 - \frac{F_m}{m})/k_B T)}\right]^m, \tag{81}$$

with the constraint of conservation of the total mole fraction X as

$$X = \sum_{m=1}^{\infty} X_m. \tag{82}$$

In Equation (81), X_1 is the mole fraction of unaggregated polyzwitterion chains and F_1 is given by Equation (32) by replacing v_d by v_{dd}. F_m is given by Equation (80) by replacing n_{eff} by m. In the context of aggregation equilibrium depicted in Equation (81), the constant term in Equation (80) is not arbitrary. We choose this constant term such that $F_m \to F_1$ for $m = 1$ in order to comply with the constraint in Equation (82), $X_{m=1} = X_1$. This yields

$$\frac{1}{k_B T}\left(F_1 - \frac{F_m}{m}\right) = \left(1 - \frac{1}{m}\right)\Theta, \tag{83}$$

where Θ follows from Equation (32) (with v_d replaced by v_{dd}), and Equation (80), as

$$\Theta = \frac{\epsilon}{2} + (2.375 - \frac{5}{2}a^{2/5}\gamma^{1/5})(\frac{1}{2} - \chi + \frac{v_{dd}}{2})^{2/5} N_e^{1/5}. \tag{84}$$

Substitution of Equation (83) in Equation (81) gives

$$X_m = m\left(X_1 e^{\Theta}\right)^m e^{-\Theta}. \tag{85}$$

This indicates that the approximate value of the critical aggregation concentration (CAC) is

$$\text{CAC} = e^{-\Theta}. \tag{86}$$

The convenient form of X_m given by Equation (85) enables analytical derivation of X_1, the average number of chains and the number of chains with the maximum propensity in the microgels. Substituting Equation (85) in Equation (82), we get

$$X = \sum_{m=1}^{\infty} X_m = \sum_{m=1}^{\infty} m(X_1 e^{\Theta})^m e^{-\Theta} = \frac{X}{(1 - X_1 e^{\Theta})^2}. \tag{87}$$

Solving the quadratic equation for X_1 in terms of X and Θ in Equation (87), we obtain

$$X_1 = \frac{(1 + 2Xe^{\Theta}) - \sqrt{1 + 4Xe^{\Theta}}}{2Xe^{2\Theta}}. \tag{88}$$

4.4. Representative Results

For the purpose of illustrating the general features of the dependence of X_m on the number of chains in the microgel on the polyzwitterion concentration c and monovalent salt concentration c_s, we give the following results. In Equation (84), Θ depends on v_{dd} and ϵ, which are c_s dependent, and N $(= N_e/\gamma)$. By choosing $a = 1, \gamma = 0.1, N_e = 50, \chi = 0$, $\ell_B = 0.7$ nm, $p = 1$ nm, $\ell = 1$ nm, and $\kappa\ell = 2.26\sqrt{c_s}$, v_{dd} is plotted in Figure 4a as a function of c_s in molarity. For the antiparallel quadrupole, we choose $\ell_B = 0.7$ nm, $p = 1$ nm, and $r_0 = 0.25$ nm, and ϵ, given by $(\ell_B p^2/r_0^3)(1 + \kappa r_0)\exp(-\kappa r_0)$, is given in Figure 4b as a function of c_s. For the above choice of parameter values, the c_s dependence of Θ is given in Figure 4c.

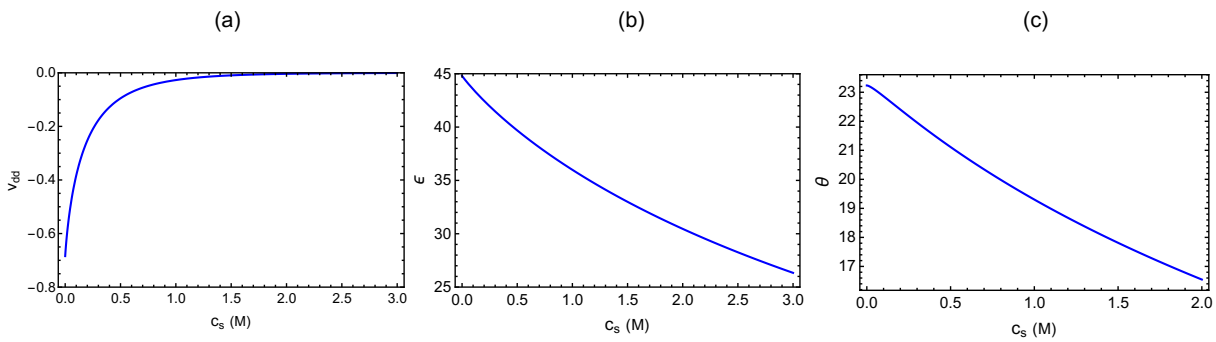

Figure 4. Dependence on salt concentration c_s of (**a**) v_{dd}, (**b**) ϵ, and (**c**) Θ.

For $c_s = 0.25$ M, the dependence of the mole fraction of unaggregated chains X_1 on the total mole fraction X of polyzwitterion chains is given in Figure 5a. The occurrence of CAC ($e^{-\Theta}$) is evident from this figure. Considering poly(sulfobetaine methacrylate) as a typical polyzwitterion, with $N = 512$ and $M_w = 180,216$ g/mol, the mole fraction of the polymer is related to its concentration c in g/L as $X = 10^{-7} = c$. The distribution of X_m on m for $c_s = 0.25$ M and $c = 1$ g/L is displayed in Figure 5b exhibiting the spontaneous selection of finite-sized microgels with a maximum around $m = 20$. The dependence of X_m on c (1.0, 0.5, 0.1 g/L) at the fixed salt concentration $c_s = 0.25$ M is portrayed in Figure 6a. At lower polyzwitterion concentrations, the propensity of formation of microgels is lower with the corresponding microgel decreasing continuously. The dependence of X_m on c_s is illustrated in Figure 6b at $c = 1$ g/L for $c_s = 0.25$ M, 0.5 M, and 1.0 M. The microgels are constituted by smaller number of chains as the salt concentration increases. The above quantitative predictions on the self-assembly of polyzwitterion microgels can be tailored to various polyzwitterion systems by choosing appropriate values of the system-dependent parameters such as the dipole moment.

Using Equation (85) for X_m at $X >$ CAC, X_m simplifies to

$$X_m \simeq m\exp(-\frac{m}{\sqrt{Xe^{\Theta}}} - \Theta), \tag{89}$$

so that $\partial X_m/\partial m = 0$ yields the number of chains in the microgel with maximum probability as

$$m_{max} = \sqrt{X}e^{\Theta/2}, \tag{90}$$

and the average number of chains in the microgel as

$$\langle m\rangle = 2m_{max} = 2\sqrt{X}e^{\Theta/2}. \tag{91}$$

Furthermore, taking the polyzwitterion volume fraction in the aggregate (microgel) as

$$\phi_{agg} = \frac{\langle m\rangle N_e \ell^3}{\frac{4}{3}\pi R_{g,agg}^3}, \tag{92}$$

where $R_{g,agg}$ is the average radius of gyration of the aggregate. Substituting ϕ_{agg} from Equation (79) in the above equation, we get

$$R_{g,agg} = (\frac{3}{2\pi})^{1/3} e^{\Theta/6} (\frac{1}{2} - \chi_{eff})^{1/5} N_e^{3/5} \ell X^{1/6}. \tag{93}$$

Hence the radius of gyration of the aggregate is proportional to the one-sixth power of polyelectrolyte concentration at all salt levels of self-assembly,

$$R_{g,agg} \sim c^{1/6}, \tag{94}$$

with the prefactor proportional to the radius of gyration of a single isolated strand under the same experimental conditions of microgel formation. The above theoretically derived exponent 1/6 for polyzwitterion microgels has earlier been implicated in the contexts of the slow mode in salt-free polyelectrolyte solutions [40] and physical polyzwitterions [30] arising from counterion binding to polyelectrolytes. These references provide experimental validation of the predictions from the present theory. The above scaling behavior appears to be universal for all associative charged macromolecular systems.

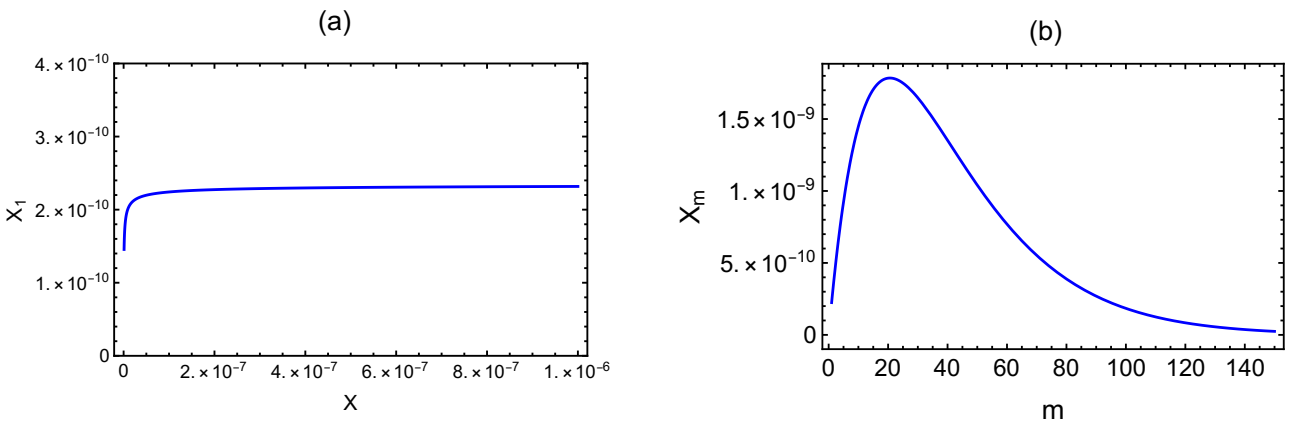

Figure 5. (**a**) Dependence of the mole fraction X_1 of unaggregated polyzwitterions on the total mole fraction of the polyzwitterion chains. (**b**) Distribution of the mole fraction of microgels containing m chains on m for $c = 1$ g/L and $c_s = 0.25$ M.

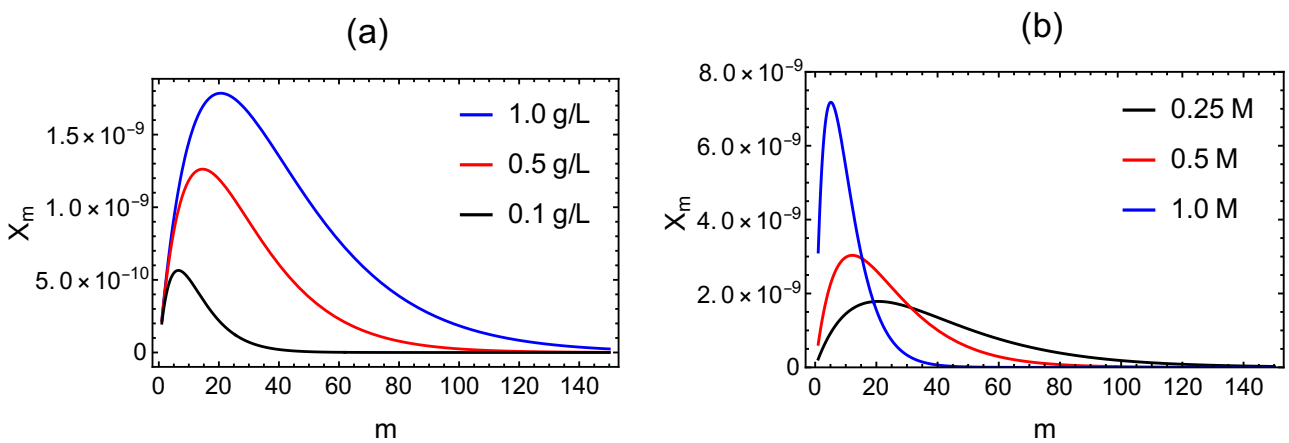

Figure 6. (**a**) Polyzwitterion concentration dependence of the distribution of the mole fraction of microgels containing m chains on m for $c = 1.0$, 0.5, and 0.1 g/L and $c_s = 0.25$ M. (**b**) Salt concentration dependence of the distribution of the mole fraction of microgels containing m chains on m for $c_s = 0.25$, 0.5, and 1.0 M and $c = 1.0$ g/L.

5. Swelling Equilibrium and Internal Dynamics of Polyzwitterion Gels

When polyzwitterion molecules in a solution at concentrations above the overlap concentration are allowed to form permanent chemical crosslinks, such gels can exhibit rich behavior encompassing both the high-temperature and low-temperature attributes described in Introduction.

5.1. Swelling Equilibrium

The derivation given in Section 4 is valid for the present situation as well, where N_c is the number of permanent crosslinks instead of physical quadrupoles (which might contribute to additional physical crosslinks). Therefore, the swelling equilibrium is given by Equation (78) as

$$\phi = \frac{\phi_0^{2/5}}{N_e^{3/5}(\frac{1}{2} - \chi_{eff})^{3/5}}, \tag{95}$$

where

$$\chi_{eff} = \chi - \frac{1}{2} v_{dd}, \tag{96}$$

for the experimental conditions that allow random orientations of the zwitterion groups, and

$$\chi_{eff} = \chi - \frac{1}{2} v_d, \tag{97}$$

for conditions where quenched quadrupoles are preferred. Since the quantitative consequences of $v_d \sim p^2$ and $v_{dd} \sim p^4$ can be significant, the volume phase transitions of chemically cross-linked polyzwitterion gels and their response to externally imposed stimuli such electric fields, mechanical forces, and added salt, can be quite different for the above two scenarios. While these issues are not addressed in the present paper, such a premise is of interest for future considerations.

5.2. Internal Dynamics

The displacement vector of the gel is a fluctuating quantity, shich can be quantified, for example, by a combination dynamic light scattering (DLS) experiments and gel elasticity theory. The displacement vector is directly proportional to to the end-to-end distance vector $\mathbf{X}(N_e, t)$ of the elastically active strands of N_e monomers in the gel. As already shown above in Equations (46) and (52), the time correlation function of $\mathbf{X}(N_e, t)$ is

$$\langle \mathbf{X}(t) \cdot \mathbf{X}(0) \rangle \sim \exp(-\frac{t}{\tau_0 N_e^x}), \tag{98}$$

where τ_0 absorbs all numerical prefactors and

$$x = \begin{cases} 2\nu + 1 & \text{Rouse} \\ 3\nu & \text{Zimm} \end{cases} \tag{99}$$

In almost all chemically cross-linked gels, N_e of all elastically active strands is not the same. For weakly cross-linked gels, it is well known that N_e is distributed according to the exponential [54],

$$P(N_e) = e^{-kN_e}, \tag{100}$$

where k is the rate of the cross-linking reaction. In fact, even if the segments between two adjacent cross-links were to locally organize into vitrimer-like dynamically associated structures, the form of Equation (100) is preserved with k depending on the local dynamical details. The electric field ($\mathbf{E}$) correlation function $g_1(t)$ measured in DLS is the superposition of Equations (98) and (100),

$$g_1(t) \sim \int dN_e \, e^{-kN_e - \frac{t}{\tau_0 N_e^x}} \sim e^{-(\frac{t}{\tau})^\beta}, \tag{101}$$

where τ is the net characteristic time that compounds all hierarchical relaxation times for strands with varying N_e values, and β is a stretched exponent,

$$\beta = \frac{1}{1+x}. \tag{102}$$

If hydrodynamic interactions are absent, then the Rouse dynamics is applicable and we get from Equation (99),

$$\beta = \frac{1}{2\nu+2}. \tag{103}$$

On the other hand, if the gel meshes are widely open to allow hydrodynamic interaction without significant screening, the Zimm dynamics is applicable so that

$$\beta = \frac{1}{3\nu+1}. \tag{104}$$

For polyzwitterion gels, where the local polymer concentration is rather high, we expect that the hydrodynamic interaction is screened so that the Rouse dynamics is applicable. As already described, when the quadrupole formation is prevalent at low salt concnetrations, $\nu = 1/3$ so that $\beta = 8/3$. On the other hand, if the formation of quadrupoles is weakened by adding salt, and since the strands between crosslinks are not too long to allow significant excluded volumere swelling, we expect $\nu \simeq 1/2$ so that $\beta = 1/3$. Thus we anticipate a crossover from $\beta = 8/3$ to $\beta = 1/3$ as c_s is increased for the hierarchical internal dynamics of polyzwitterion gels as sketched in Figure 7.

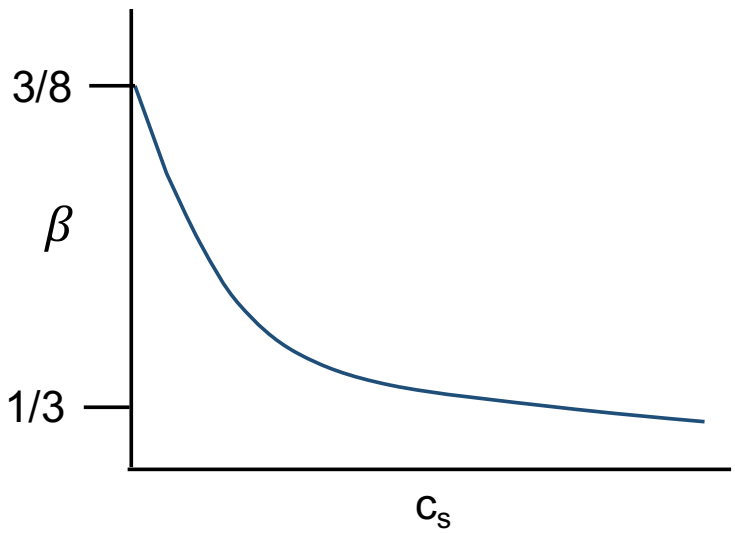

Figure 7. The stretched exponent β for hierarchical internal dynamics of polyzwitterion gels is $8/3$ for salt-free limit and it decreases to $1/3$ as the concentration of added salt increases.

6. Conclusions

The incipient ability of dipolar zwitterion monomers of polyzwitterions to associate results in a broad range of properties unlike the situation with uniformly charged polyelectrolytes. Even though there have previously been several theoretical attempts to treat polyzwitterions, they assume that the dipolar zwitterionic moieties are randomly oriented. In reality, this assumption can be valid only if the temperature is extremely high or the concentration of added low molar mass electrolyte is very high. In order to be relevant to practical experimental systems, it is necessary to treat drastic deviations from the random-orientation paradigm. The theory presented here is a new paradigm for treating the behavior of polyzwitterions. Here, the non-random orientations of zwitterionic groups into quenched conformations are explicitly treated using statistical mechanics and field-theoretic methods.

In the present theory, two regimes have been identified for the rotational degree of freedom associated with the zwitterion dipoles. In the high-temperature regime, the dipoles are randomly oriented. In the low-temperature regime, the dipole orientations are quenched resulting in quadrupoles. In developing a theoretical formulation for polyzwitterion solutions, we have accounted for the spontaneous formation of quadrupoles in the low-temperature regime.

In the present mean field theory of polyzwitterion systems, we have derived closed-form formulas for (a) the size and dynamics of isolated chains in dilute solutions, (b) self-assembly of mesomorphic microgels in semidilute solutions, and (c) swelling equilibrium and hierarchical internal dynamics of chemically cross-linked polyzwitterion gels.

The general picture that emerges from the considerations in the present work is sketched in Figure 8. The key experimental variables can be temperature or salt concentration or pH, in addition to the polyzwitterion concentration. In this figure, the ordinate is any one of the variables: temperature T, salt concentration c_s, and pH of the solution. In general, the phase diagram is multi-dimensional. In order to emphasize this aspect of multi-dimensionality, we have inserted the slanted lines denoting pH and c_s by focussing on the variable T (orthogonal to the abscissa). Therefore, as an example of the ordinate variable, let the temperature be the experimental handle to explore the behavior of polyzwitterions. In extremely dilute solutions and at high temperatures, individual polyzwitterion chains exist as expanded coils. When the temperature is lowered, the chain undergoes coil-to-globule transition. However, the globule exhibits the anti-polyelectrolyte effect of expanding into the coil conformation upon addition of salt.

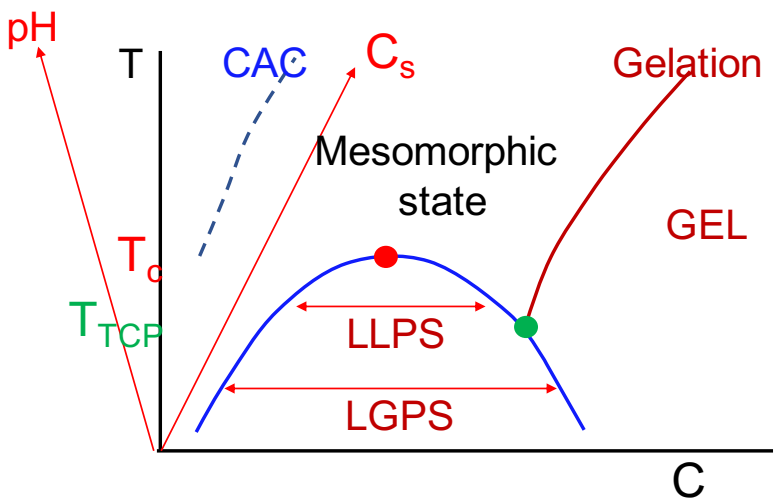

Figure 8. Generalized phase diagram for polyzwitterion solutions. The ordinate is any one of the variables: temperature T, salt concentration c_s, and pH of the solution. In general, the phase diagram is multi-dimensional. In order to emphasize this aspect of multi-dimensionality, we have inserted the slanted lines denoting pH and c_s by focussing on the variable T (orthogonal to the abscissa denoting the polymer concentration).

In the high-temperature region, but not too high, as the polymer concentration is increased, the polyzwitterion chains spontaneously aggregate into mesomorphic microgels. In between the dilute regime and the mesomorphic state, there is a line denoting the critical aggregation concentration necessary for the formation of the microgels. Upon further increase in polymer concentration, the mesmorphic state becomes a gel if the polymer concentration is higher than that corresponding to the gelation threshold.

For intermediate polymer concentrations, when the temperature is lowered, dipolar correlations result in quadrupoles and multipoles generating structural heterogeneity that interferes with fluctuations in the local polymer concentration. Eventually, as the temperature is lowered, a critical temperature T_c is reached below which liquid-liquid

phase separation (LLPS) occurs. At temperatures lower than T_c, a tricritical point can emerge at the temperature T_{TCT} at which the gel line meets the coexistence curve. For temperatures below T_{TCT}, liquid-gel phase separation (LGPS) occurs.

In the above general context of the rich phase behavior, we have only addressed in this paper the behaviors outside the critical point and the coexistence curve. Since the present work shows that the dipolar associations in polyzwitterion systems lead to significantly rich consequences in contrast with considerations where dipoles are assumed to be randomly oriented, such dipolar associations are expected to play a major role in the construction of LLPS and LGPS phase behaviors.

This theory makes many predictions on (a) the structure and dynamics of polyzwitterions in dilute solutions, (b) emergence of a spontaneous formation of mesomorphic microgel aggregates and their size distribution, and (c) swelling equilibria and hierarchical internal dynamics of polyzwitterion gels. These predictions open a new avenue of experiments toward critical assessments of theoretical predictions, more fundamental understanding of polyzwitterion behavior, and potential applications.in health care industry. Furthermore, since the present theory is only based on mean-field arguments, treatment of concentration fluctuations is of immediate future interest.

It must be mentioned that the dipolar behaviors addressed in the present work are also present in biological macromolecules such as intrinsically disordered proteins. Extension of the present theory to such broader situations is of considerable future interest.

Funding: Acknowledgement is made to the National Science Foundation (Grant No. DMR 2309539) and AFOSR (Grant No. FA9550-23-1-0584).

Institutional Review Board Statement: Not applicable.

Informed Consent Statement: Not applicable.

Data Availability Statement: The data presented in this study are openly available in article.

Acknowledgments: It is a great pleasure to thank Di Jia, Shibananda Das, Siao-Fong Li, and Yeseul Lee for stimulating discussions.

Conflicts of Interest: The author declares no conflict of interest.

References

1. Muthukumar, M. *Physics of Charged Macromolecules: Synthetic and Biological Systems*; Cambridge University Press: Cambridge, UK, 2023.
2. Lowe, A.B.; McCormick, C.L. Synthesis and solution properties of zwitterionic polymers. *Chem. Rev.* **2002**, *102*, 4177–4190. [CrossRef] [PubMed]
3. Kudaibergenov, S.; Jaeger, W.; Laschewsky, A. Polymeric betaines: Synthesis, characterization, and application. In *Supramolecular Polymers Polymeric Betaines Oligomers*; Springer: Berlin/Heidelberg, Germany, 2006; pp. 157–224.
4. Laschewsky, A. Structures and synthesis of zwitterionic polymers. *Polymers* **2014**, *6*, 1544–1601. [CrossRef]
5. Neitzel, A.E.; De Hoe, G.X.; Tirrell, M.V. Expanding the structural diversity of polyelectrolyte complexes and polyzwitterions. *Curr. Opin. Solid State Mater. Sci.* **2021**, *25*, 100897. [CrossRef]
6. Hildebrand, V.; Laschewsky, A.; Panach, M.; Manuller-Buschbaum, P.; Papadakis, C.M. Effect of the zwitterion structure on the thermo-responsive behaviour of poly (sulfobetaine methacrylates). *Polym. Chem.* **2017**, *8*, 310–322. [CrossRef]
7. Zheng, L.; Sundaram, H.S.; Wei, Z.; Li, C.; Yuan, Z. Applications of zwitterionic polymers. *React. Funct. Polym.* **2017**, *118*, 51–61. [CrossRef]
8. Wielema, T.A.; Engberts, J.B. Zwitterionic polymers-II. Synthesis of a novel series of poly (vinylbetaines) and the effect of the polymeric structure on the solubility behaviour in water. *Eur. Polym. J.* **1990**, *26*, 415–421. [CrossRef]
9. Niskanen, J.; Tenhu, H. How to manipulate the upper critical solution temperature (UCST)? *Polym. Chem.* **2017**, *8*, 220–232. [CrossRef]
10. Guo, S.; Quintana, R.; Cirelli, M.; Toa, Z.S.D.; Arjunan Vasantha, V.; Kooij, E.S.; JaLnczewski, D.; Vancso, G.J. Brush swelling and attachment strength of barnacle adhesion protein on zwitterionic polymer films as a function of macromolecular structure. *Langmuir* **2019**, *35*, 8085–8094. [CrossRef] [PubMed]
11. Mary, P.; Bendejacq, D.D.; Labeau, M.-P.; Dupuis, P. Reconciling low-and high-salt solution behavior of sulfobetaine polyzwitterions. *J. Phys. Chem. B* **2007**, *111*, 7767–7777. [CrossRef]
12. Shao, Q.; Mi, L.; Han, X.; Bai, T.; Liu, S.; Li, Y.; Jiang, S. Differences in Cationic and Anionic Charge Densities Dictate Zwitterionic Associations and Stimuli Responses. *J. Phys. Chem. B* **2014**, *118*, 6956–6962. [CrossRef]

13. Tuzar, Z.; Pospisil, H.; Plestil, J.; Lowe, A.B.; Baines, F.L.; Billingham, N.C.; Armes, S.P. Micelles of Hydrophilic–Hydrophobic Poly(sulfobetaine)-Based Block Copolymers. *J. Phys. Chem. B* **2003**, *107*, 7982–7986. [CrossRef]
14. Izumrudov, V.A.; Domashenko, N.I.; Zhiryakova, M.V.; Davydova, O.V. Interpolyelectrolyte Reactions in Solutions of Polycarboxybetaines, 2: Influence of Alkyl Spacer in the Betaine Moieties on Complexing with Polyanions. *J. Phys. Chem. B* **2005**, *109*, 17391–17399. [CrossRef] [PubMed]
15. Bohrisch, J.; Grosche, O.; Wendler, U.; Jaeger, W.; Engelhardt, H. Electroosmotic mobility and aggregation phenomena of model polymers with permanent cationic groups. Macromol. *Chem. Phys.* **2000**, *201*, 447–452.
16. Wielema, T.A.; Engberts, J.B.F.N. Zwitterionic polymers. 1. Synthesis of a novel series of poly(vinylsulfobetaines) -effect of structure of polymer on solubility in water. *Eur. Polym. J.* **1987**, *23*, 947–950. [CrossRef]
17. Bonte, N.; Laschewsky, A. Zwitterionic polymers with carbobetaine moieties. *Polymer* **1996**, *37*, 2011–2019. [CrossRef]
18. Huglin, M.B.; Radwan, M.A. Unperturbed dimensions of a zwitterionic polymethacrylate. *Polym. Int.* **1991**, *26*, 97–104. [CrossRef]
19. Schulz, D.N.; Peiffer, D.G.; Agarwal, P.K.; Larabee, J.; Kaladas, J.J.; Soni, L.; Handwerker, B.; Garner, R.T. Phase behaviour and solution properties of sulphobetaine polymers. *Polymer* **1986**, *27*, 1734. [CrossRef]
20. Salamone, J.C.; Volksen, W.; Olson, A.P.; Israel, S.C. Aqueous solution properties of a poly(vinyl imidazolium sulphobetaine). *Polymer* **1978**, *19*, 1157. [CrossRef]
21. Soto, V.M.M.; Galin, J.C. Poly(sulphopropylbetaines): 2. Dilute solution properties. *Polymer* **1984**, *25*, 254–262. [CrossRef]
22. Kato, T.; Takahashi, A. Excluded volume effects of sulphobetaine polymers. *Berichte Bunsenges. Phys. Chem.* **1996**, *100*, 784–787. [CrossRef]
23. Kudaibergenov, S.E. Polyampholytes. In *Encyclopedia of Polymer Science and Technology*; John Wiley & Sons: New York, NY, USA, 2002.
24. Niu, A.; Liaw, D.; Sang, H.; Wu, C. Light-Scattering Study of a Zwitterionic Polycarboxybetaine in Aqueous Solution. *Macromolecules* **2000**, *33*, 3492–3494. [CrossRef]
25. Liaw, D.; Huang, C. Dilute solution properties of poly(3-dimethyl acryloyloxyethyl ammonium propiolactone). *Polymer* **1997**, *38*, 6355–6362. [CrossRef]
26. Matsuda, Y.; Kobayashi, M.; Annaka, M.; Ishihara, K.; Takahara, A. Dimension of Poly(2-methacryloyloxyethyl phosphorylcholine) in Aqueous Solutions with Various Ionic Strength. *Chem. Lett.* **2006**, *35*, 1310–1311. [CrossRef]
27. Morozova, S.; Hu, G.; Emrick, T.; Muthukumar, M. Influence of dipole orientation on solution properties of polyzwitterions. *ACS Macro Lett.* **2016**, *5*, 118–122. [CrossRef] [PubMed]
28. Wang, F.; Yang, J.; Zhao, J. Understanding anti-polyelectrolyte behavior of a welldefined polyzwitterion at the single-chain level. *Polym. Int.* **2015**, *64*, 999–1005. [CrossRef]
29. Pickett, P.D.; Ma, Y.; Lueckheide, M.; Mao, Y.; Prabhu, V.M. Temperature dependent single-chain structure of poly [3-(acrylamidopropyl-dimethyl-ammonium) propyl- 1-sulfonate] via small-angle neutron scattering. *J. Chem. Phys.* **2022**, *156*, 214904. [CrossRef] [PubMed]
30. Jia, D.; Muthukumar, M. Dipole-driven interlude of mesomorphism in polyelectrolyte solutions. *Proc. Natl. Acad. Sci. USA* **2022**, *119*, e2204163119. [CrossRef]
31. Georgiev, G.S.; Kamenska, E.B.; Vassileva, E.D.; Kamenova, I.A.; Georgieva, V.T.; Iliev, S.B.; Ivanov, I.A. Self-Assembly, Antipolyelectrolyte Effect, and NonbiofoulingProperties of Polyzwitterions. *Biomacromolecules* **2006**, *7*, 1329–1334. [CrossRef]
32. Bredas, J.R.; Chance, R.R.; Silbey, R. Head-Head Interactionsin Zwitterionic Associating Polymers. *Macromolecules* **1988**, *21*, 1633–1639. [CrossRef]
33. Tsonchev, S.; Troisi, A.; Schatz, G.C.; Ratner, M.A. All-Atom Numerical Studies of Self-Assembly of Zwitterionic Peptide Amphiphiles. *J. Phys. Chem. B* **2004**, *108*, 15278–15284. [CrossRef]
34. Dobrynin, A.V.; Colby, R.H.; Rubinstein, M. Polyampholytes. *J. Polym. Sci. Part B Polym. Phys.* **2004**, *42*, 3513–3538. [CrossRef]
35. Muthukumar, M. Localized structures of polymers with long-range interactions. *J. Chem. Phys.* **1996**, *104*, 691–700. [CrossRef]
36. Bratko, D.; Chakraborty, A. A numerical study of polyampholyte configuration. *J. Phys. Chem.* **1996**, *100*, 1164–1173. [CrossRef]
37. Higgs, P.G.; Joanny, J. Theory of polyampholyte solutions. *J. Chem. Phys.* **1991**, *94*, 1543. [CrossRef]
38. Kumar, R.; Fredrickson, G.H. Theory of polyzwitterion conformations. *J. Chem. Phys.* **2009**, *131*, 104901. [CrossRef]
39. Bhattacharjee, A.; Kundu, P.; Dua, A. Self-Consistent Theory of Structures and Transitions in Weak Polyampholytes. *Macromol. Theory Simul.* **2011**, *20*, 75–84. [CrossRef]
40. Muthukumar, M. Ordinary-extraordinary transition in dynamics of solutions of charged macromolecules. *Proc. Natl. Acad. Sci. USA* **2016**, *113*, 12627–12632. [CrossRef]
41. Mahalik, J.P.; Muthukumar, M. Simulation of self-assembly of polyzwitterions into vesicles. *J. Chem. Phys.* **2016**, *145*, 074907. [CrossRef] [PubMed]
42. Gordievskaya, Y.D.; Budkov, Y.A.; Kramarenko, E.Y. An interplay of electrostatic and excluded volume interactions in the conformational behavior of a dipolar chain: Theory and computer simulations. *Soft Matter* **2018**, *14*, 3232–3235. [CrossRef]
43. Gordievskaya, Y.D.; Kramarenko, E.Y. Conformational behavior of a semiflexible dipolar chain with a variable relative size of charged groups via molecular dynamics simulations. *Soft Matter* **2019**, *15*, 6073–6085. [CrossRef]
44. Muthukumar, M. Adsorption of a polyelectrolyte chain to a charged surface. *J. Chem. Phys.* **1987**, *86*, 7230–7235. [CrossRef]
45. Doi, M.; Edwards, S.F. *The Theory of Polymer Dynamics*; Clarendon Press: Oxford, UK, 1986.
46. Tanaka, F. Theory of thermoreversible gelation. *Macromolecules* **1989**, *22*, 1988–1994. [CrossRef]

47. Semenov, A.N.; Rubinstein, M. Thermoreversible Gelation in Solutions of Associative Polymers. 1. Statics. *Macromolecules* **1998**, *31*, 1373–1385. [CrossRef]
48. Flory, P.J. *Principles of Polymer Chemistry*; Cornell University Press: Ithaca, NY, USA, 1953.
49. Dusek, K.; Patterson, D. Transition in swollen polymer networks induced by intramolecular condensation. *J. Polym. Sci. Part A-2* **1968**, *6*, 1209–1216. [CrossRef]
50. Tanaka, T. Collapse of gels and the critical end point. *Phys. Rev. Lett.* **1978**, *40*, 820–823. [CrossRef]
51. Shibayama, M.; Tanaka, T. *Responsive Gels: Volume Transitions I*; Dusek, K., Ed.; Springer: Berlin/Heidelberg, Germany, 1993; pp. 1–62.
52. Jia, D.; Muthukumar, M. Theory of charged gels; Swelling, elasticity, and dynamics. *Gels* **2021**, *7*, 49. [CrossRef]
53. Israelachvili, J.N. *Intermolecular and Surface Forces*; Academic Press: Cambridge, MA, USA, 2011.
54. Sommer, J.-U. On the dynamics of moderately crosslinked networks. *J. Chem. Phys.* **1991**, *95*, 1316–1317. [CrossRef]